*Research Inventy: International Journal of Engineering And Science*
*Vol.15, Issue 7 (July 2025), PP 47-56*
*Issn (e): 2278-4721, Issn (p):2319-6483, www.researchinventy.com*

# Mechanical, antibacterial and in-vitro bioactivity of ZnO-doped $Na_2O$-Cao-$SiO_2$ glass-ceramic system using waste soda-lime-silica glass.

BabatundeOji[a]., Ebenezer TayoAliu[a] and Olusola Joseph Ajayi[a]
[a] *Department of Glass and Ceramic Technology, Federal Polytechnic, P.M.B 5351, Ado-Ekiti, Nigeria.*
**Corresponding Author*

***Abstract***
*This study examines the mechanical properties, antibacterial performance, and in vitro bioactivity of ZnO-doped $Na_2O$–$CaO$–$SiO_2$ glass-ceramic system developed from waste soda-lime-silica glass. It aims to address the environmental concerns associated with waste glass accumulation by valorizing it into scientifically and economically valuable materials. The waste glass was collected from dumpsites, cleaned by washing to remove impurities and dried under ambient atmospheric conditions to eliminate residual moisture. The dried glass was manually crushed, milled in a jar mill for 12 hours, and sieved through a 230-mesh (125 µm) sieve to ensure uniform particle sizes. Samples were prepared by mixing raw materials in varying weight ratios of ZnO to base glass (0:100, 5:95, 10:90, 15:85, and 20:80), with polyvinyl alcohol added as a binder. The mixtures were compacted at 200 MPa using a uniaxial press and sintered at 1000°C for 30 minutes in a microwave furnace before characterization were done using hardness and compression testing, XRD, SEM/EDS, XRF and antibacterial assays. The mechanical testing revealed a non-linear decrease in hardness and compressive strength with increasing ZnO content, supported by the pre-in vitro XRD and SEM/EDS analyses showing phase compositions and microstructural changes consistent with these trends. In vitro bioactivity was confirmed by the formation of hydroxyapatite (HA) on sample surfaces, indicated by distinct HA peaks in post-in-vitro XRD patterns and the presence of well-defined apatite layers in SEM images. XRF analysis also shows increased calcium levels in post-immersion, supporting HA formation while antibacterial testing revealed that the samples exhibited strain-dependent antimicrobial efficacy, further highlighting their potential for biomedical applications.*

***Keywords:*** *Waste glass, Bioactive, Antibacterial, Hydroxyapatite, Sintering*

---

Date of Submission: 06-07-2025 Date of acceptance: 17-07-2025

---

## I. INTRODUCTION

Solid waste management remains a critical environmental issue, with waste glass constituting a significant portion due to its non-biodegradable nature. Disposal of waste glass in landfills not only presents environmental hazards but also consumes valuable land resources that could be allocated to economically productive uses. Although rapid industrial development has spurred interest in glass recycling, substantial barriers remain in optimizing its economic and societal benefits to support sustainable industrial advancement [Chong*et al.,* 2011].

Glass is a ubiquitous material with diverse applications across industries such as construction, interior design, pharmaceuticals, automotive manufacturing, laboratory equipment, and food and beverage packaging. This widespread use has resulted in the generation of large volumes of waste glass [Hsiang et al., 2019, Li*et al.,* 2019]. For instance, Jani and Hogland, 2014reported that the United States generated approximately 11.5 million tons of waste glass in 2010, with a recycling rate of only 27%. Similarly, European commission's(2010)also reported that in Europe 4.1 million tons of waste glass were produced in 2008, with 60% recycled. Wang, (2020)also reported that by 2018, global glass production reached an estimated 130 million tons, yet only 20% was recycled. Without effective recycling strategies, the cumulative accumulation of waste glass poses serious environmental threats, underscoring the need for alternative innovative recycling approaches and value-added applications.

Recycling waste glass presents several advantages, including energy conservation, cost reduction, environmental sustainability, natural resource preservation, and a decrease in greenhouse gas emissions (Husseine*t al.,* 2022). Prior researchers have demonstrated the feasibility of integrating recycled glass into construction materials, polymer composites, ceramics, concrete, and foam glass (Castro *et al.,* 2013; Robert *et*

*al.,* 2021; Lopez *et al.,* 2012;Asokan*et al.,* 2009;Derweesh 2019;Pahlevani&Sahajwalla 2018;Akinyele*et al.,* 2020;Assefi*et al.,* 2021).

Beyond convectional applications, waste glass also shows significant potential as a precursor for bioactive and antimicrobial materials, particularly in biomedical contexts. Bioactive glasses are capable of forming strong bonds with bone tissue through a sequence of reactions involving ion exchange, hydrolysis, and the development of a hydroxycarbonate apatite (HCA) layer. The elemental composition of typical waste glass comprising $SiO_2$, $Na_2O$, CaO, and $P_2O_5$ is similar to that of bioactive glasses, enabling hydroxyapatite formation and the release of biologically relevant ions such as Si, Ca, P, and Na, which promote Osseo integration (Hoppe *et al.,* 2011;Mahboubizadeh*et al.,* 2023).In parallel, the demand for antimicrobial surfaces in clinical, industrial, and domestic environments, especially those prone to moisture, continues to grow due to increasing concerns over microbial contamination linked to significant morbidity and mortality rate (Onaizi*et al.,* 2011; Anderson 2010; Özcan*et al.,* 2017). Antimicrobial coatings are generally formulated with agents like $TiO_2$, ZnO, Ag, and Cu, which inhibit microbial proliferation on glazed surfaces (Noguera*et al*., 2010; Mio *et al.,* 2014; Chanrawangyot*et al*., 2017; Maryan*et al.,* 2020). Due to its inherent hardness, chemical durability, and smooth surface, waste glass presents a promising substrate for such antimicrobial applications. However, existing research has predominantly focused on ceramic-based systems, with limited exploration of waste glass as a viable alternative.

This study therefore investigates the potential of developing functionalized waste glass as a bioactive and antibacterial material. Waste soda-lime-silica glass was processed via milling and sieving, then blended with ZnO particles and subjected to microwave sintering. The mechanical, bioactive, and antibacterial properties of the resulting materials were thereafter evaluated. Findings indicate that the developed functionalized glass-ceramics exhibits favorable properties suitable for sterilization surfaces and potential biomedical implant applications.

## II. MATERIALS AND METHOD

### 2.1 Materials

The materials employed in this study included waste soda-lime-silica glass, zinc oxide (ZnO), distilled water, and polyvinyl alcohol (PVA). The waste glass was sourced from discarded glasses collected within the Department of Glass and Ceramics Technology at the Federal Polytechnic, Ado-Ekiti, Nigeria. Zinc oxide and polyvinyl alcohol were procured from Pascal Chemicals, Akure, Nigeria, and were utilized in their as-received form without further modification.

### 2.2 Materials and sample preparation

The waste soda-lime glass was collected in bulk, thoroughly washed to remove surface contaminants, and subsequently air-dried under sunlight. Once dried, the glass was manually crushed into smaller fragments before being subjected to mechanical milling in a jar mill for 12 hours to achieve fine powder. The milled glass was then sieved through a 230-mesh metallurgical sieve (125 μm) to obtain particles with uniform size distribution.For sample preparation, the constituent materials were weighed according to stoichiometric requirements using a digital analytical balance and manually mixed to ensure homogeneity. Polyvinyl alcohol (PVA) was incorporated as a binder to enhance compaction. The resulting mixture was compacted into cylindrical pellets using a plastic mold under a uniaxial pressure of 200 MPa. The compacted samples were subsequently sintered in a microwave furnace at a temperature of 1000 °C with a soaking time of 30 minutes. The final products were designated as $AMG_1$, $AMG_2$, $AMG_3$, $AMG_4$, and $AMG_5$.

**Table 1:** sample designation of the developed glass-ceramics system

| samples | $AMG_1$ | $AMG_2$ | $AMG_3$ | $AMG_4$ | $AMG_5$ |
|---|---|---|---|---|---|
| **Waste glass** | 100 | 95 | 90 | 85 | 80 |
| **Zinc Oxide** | 0 | 5 | 10 | 15 | 20 |

### 2.3 Antibacterial activities of developed glass-ceramics system

The antimicrobial activity of the developed materials was assessed against selected bacterial strains, including Escherichia coli and Klebsiellapneumoniae (Gram-negative), as well as Staphylococcus aureus and Pseudomonas aeruginosa (Gram-positive). The microbial inoculum was prepared following the procedure described by Gross *et al.,* 2024involving the direct suspension of actively growing colonies in nutrient broth. The suspension was standardized to a turbidity equivalent to the 0.5 McFarland standard (approximately $1 \times 10^8$ CFU/mL), corresponding to an optical density of 0.08–0.10 at 625 nm, as measured using a UV-Vis spectrophotometer (UV-1800).Subsequently, the bacterial suspension was diluted at a ratio of 1:150 to achieve a final concentration of $1 \times 10^6$ CFU/mL. Using a sterile swab, the diluted inoculum was uniformly spread over the surface of Mueller-Hinton agar plates to ensure consistent microbial coverage. Following inoculation, the

agar plates were incubated at 37 °C for 24 hours, after which the antimicrobial efficacy was evaluated by measuring the diameters of the zones of inhibition surrounding the test samples.

### 2.4 In-vitro bioactivity of developed glass-ceramics system

To evaluate the in vitro bioactivity of the developed glass-ceramic system, an immersion test was conducted using simulated body fluid (SBF), following the standard protocol established by Kokubo and Takadama 2006. Disc-shaped specimens, each measuring approximately 20 × 5 mm, were prepared from the developedsamples designated $AMG_1$, $AMG_2$, $AMG_3$, $AMG_4$, and $AMG_5$. These discs were then immersed in pre-prepared SBF solution contained in plastic beakers.Each sample was positioned at a slight inclination within the beaker to ensure maximum surface contact with the SBF. The beakers were maintained at a constant temperature of 37 °C to simulate physiological conditions, and the immersion was sustained for a 24-hour period. Following the exposure, the samples were gently rinsed with deionized water to remove any loosely adhered particles and subsequently air-dried at room temperature.The surfaces of the treated samples were then characterized using scanning electron microscopy (SEM) and X-ray fluorescence (XRF) spectroscopy to examine the formation of apatite layers, indicative of bioactive behavior.

### 2.5 Characterization of developed glass-ceramics system

The developed samples were subjected to a series of characterization techniques to evaluate their mechanical properties, antibacterial activity, chemical composition, structural phases, and morphological features. Mechanical performance was assessed by measuring Vickers micro hardness using a Zwick/Roell Indented ZHV tester, applying a load of 19.6 g for 10 seconds to evaluate the resistance to localized plastic deformation. Compressive strength, indicative of the samples' load-bearing capacity and structural stability, was determined using a Form Test Seidner compression testing machine (Model GMBH D7940).Microstructural analysis and surface morphology were examined using a scanning electron microscope (JSM-6100 JEOL), enabling the observation of grain structure, porosity, and surface texture. Phase composition and crystallinity were investigated through X-ray diffraction (XRD) analysis, performed using a BRUKER AXS D8 Advance diffractometer equipped with Cu Kα radiation, with diffraction patterns recorded across a suitable 2θ range. Additionally, the elemental composition of the samples was determined using a portable X-ray fluorescence (PXRF) analyzer.

## III. RESULTS AND DISCUSSIONS

### 3.1 Mechanical evaluation of the developed glass-ceramics system

Figure 1 presents the hardness and compressive strength results of glass-ceramic system developed from waste soda-lime-silica glass, modified with varying concentrations of ZnO. The incorporation of 5 wt% and 10 wt% ZnO in samples $AMG_2$ and $AMG_3$, respectively, resulted in a noticeable reduction in both hardness and compressive strength relative to the undoped sample ($AMG_1$). This decline is likely due to the role of ZnO as a network modifier, where $Zn^{2+}$ ions disrupt the $SiO_2$ network, leading to the formation of non-bridging oxygen species. Such structural changes have been shown to weaken the glass matrix, as reported by Kim *et al.,* 2015. Another possible explanation could be ZnOinducing phase separation or the formation of new crystalline phases with lower intrinsic hardness than the glass network (Hanfi*et al.,* 2024). At a doping concentration of 15 wt% ZnO ($AMG_4$), there was also a marked increase in hardness compared to $AMG_2$ and $AMG_3$, potentially due to the formation of a more robust crystalline phase that enhances resistance to localized deformation. However, a further increase to 20 wt% ZnO ($AMG_5$) resulted in a decline in mechanical performance, suggesting that exceeding an optimal ZnO concentration may promote the formation of softer crystalline phases or increase the amorphous content, thereby reducing overall material strength (Thipperudrappa*et al*., 2020; Matori*et al.,* 2010)

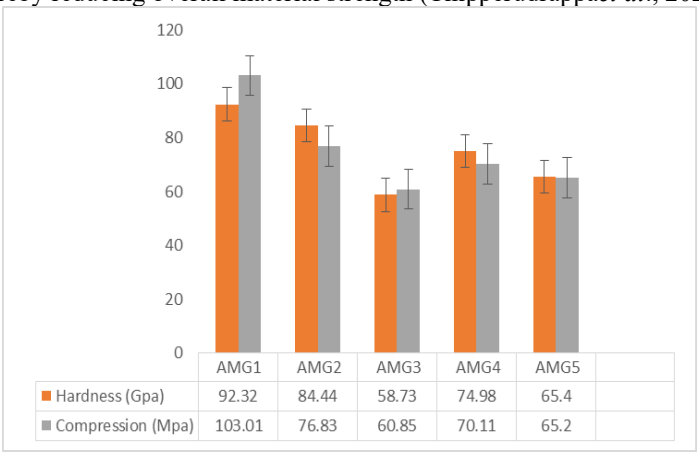


Fig. 1. Hardness and compression results of developed glass-ceramics systems

### 3.2 Pre-in-vitro XRD analysis of the developed glass-ceramics system

Figure 2 presents the superimposed pre-in-vitro X-ray diffraction (XRD) patterns of glass-ceramic system developed from waste soda-lime-silica glass with varying ZnO concentrations. The undoped sample ($AMG_1$), which exhibited the highest hardness, likely possesses a robust microstructure attributed to the synergistic presence and high crystallinity of combeite and wollastonite phases. The presence of quartz a known hard phase may further contribute to the superior mechanical strength observed in this sample (Almasri*et al.,* 2017). The observed reduction in hardness upon ZnO incorporation is potentially due to the formation of crystalline ZnO phases, which disrupt the silicate glass network and compromise its structural rigidity. While the ZnO phase may offer antibacterial benefits, it appears less effective in reinforcing mechanical strength compared to the combeite–wollastonite matrix (Effendy*et al.,* 2021; Sahu*et al.,* 2023). A decrease in the crystallinity of these key reinforcing phases would naturally lead to diminished mechanical performance (Mahdy*et al.,* 2022). The moderate increase in hardness observed in $AMG_4$ (15 wt% ZnO) may indicate an improved phase balance, where a more favorable distribution between crystalline and amorphous phases contributes to a denser and mechanically stronger structure relative to $AMG_3$. This suggests that an optimal ZnO content can enhance mechanical properties by promoting a well-integrated crystalline network phase. Conversely, the further decline in hardness in $AMG_5$ (20 wt% ZnO) is likely due to the dominance of the ZnO phase, which may inhibit the formation of the combeite–wollastonite network. The reduced intensity of the wollastonite peak, a phase known for its reinforcing effect in glass-ceramics, may also be a contributing factor to the observed decrease in mechanical strength (Hossain*et al.,* 2020; Soares*et al.,* 2018).

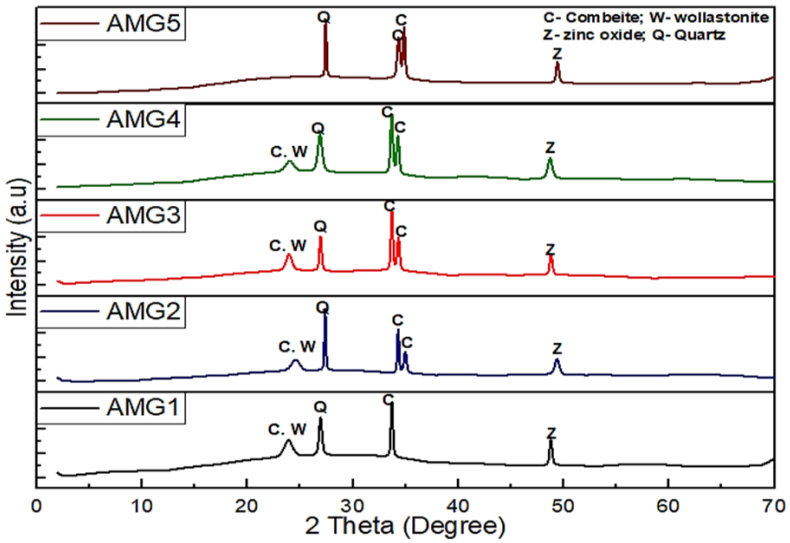


Fig. 2. XRD results of developed glass-ceramics system

### 3.3 Pre-in-vitro SEM/EDS analysis of developed glass-ceramics system

Figure 3 displays the Scanning Electron Microscopy (SEM) images and Energy Dispersive X-ray Spectroscopy (EDS) elemental analysis of glass-ceramic system developed from waste soda-lime-silica glass doped with varying concentrations of ZnO. The SEM micrograph of the undoped sample ($AMG_1$) reveals a relatively dense and well-integrated microstructure with minimal porosity, which likely contributes to its superior hardness and is consistent with the XRD results. The absence of ZnO in this sample may have promoted the development of a more homogeneous and compact glass matrix, thereby enhancing its structural rigidity. In contrast, the SEM images of ZnO-doped samples ($AMG_2$ to $AMG_5$) display significant microstructural changes, including irregular particle morphologies, localized agglomerations, and the presence of entrapped air pockets and internal voids. These features may act as stress concentrators, reducing inter-particle connectivity and adversely affecting mechanical performance, as reflected in the lower hardness and compressive strength values. The introduction of ZnO appears to induce microstructural heterogeneity that compromises both indentation resistance and load-bearing capacity. EDS elemental mapping confirms the presence of key element like Si, Na, Ca, P, Mg, Al, Zn, and K in all samples. Of particular importance is the detection of silicon, calcium, sodium, and phosphorus, elements that are crucial in the nucleation and growth of hydroxyapatite, a bioactive phase known to facilitate bone bonding in biomedical applications (Hoppe*et al.,* 2011; Hossain *et al.,* 2020).

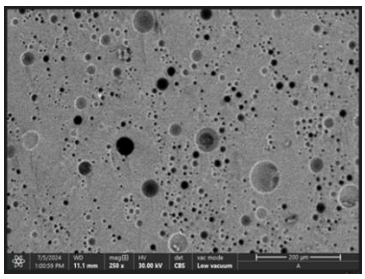

| Element symbol | Si | Na | Ca | Mg | P | K | Cl | S | Ti |
|---|---|---|---|---|---|---|---|---|---|
| Atomic Conc. | 54.42 | 21.67 | 7.19 | 6.05 | 0.82 | 0.91 | 0.96 | 0.94 | 0.52 |
| Weight Conc. | 58.79 | 17.86 | 10.33 | 5.27 | 0.91 | 0.78 | 1.22 | 1.08 | 0.90 |

($AMG_1$)

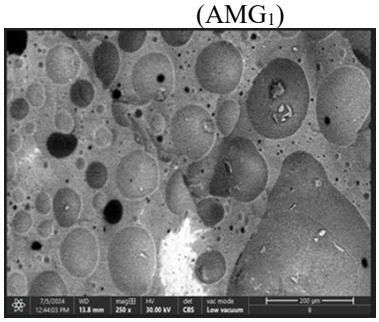

| Element symbol | Si | Na | Ca | Mg | P | K | Cl | S | Ti |
|---|---|---|---|---|---|---|---|---|---|
| Atomic Conc. | 59.68 | 21.18 | 6.88 | 6.31 | 1.06 | 0.59 | 0.66 | 1.00 | 0.16 |
| Weight Conc. | 60.33 | 17.53 | 9.92 | 5.52 | 1.19 | 0.83 | 0.84 | 1.15 | 0.27 |

($AMG_2$)

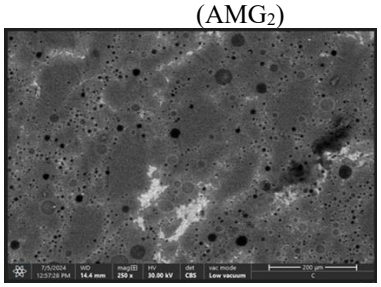

| Element symbol | Si | Na | Ca | Mg | P | K | Cl | S | Ti |
|---|---|---|---|---|---|---|---|---|---|
| Atomic Conc. | 59.36 | 24.41 | 5.37 | 4.99 | 1.09 | 0.53 | 0.49 | 1.00 | 0.00 |
| Weight Conc. | 60.77 | 20.46 | 7.84 | 4.42 | 1.23 | 0.76 | 0.64 | 1.17 | 0.00 |

($AMG_3$)

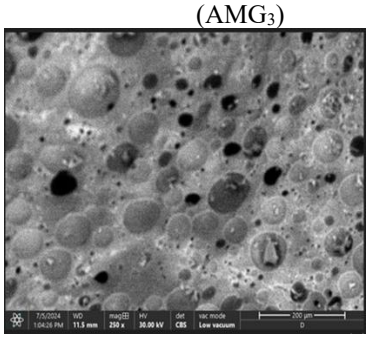

| Element symbol | Si | Na | Ca | Mg | P | K | Cl | S | Ti |
|---|---|---|---|---|---|---|---|---|---|
| Atomic Conc. | 55.72 | 23.52 | 7.35 | 4.45 | 0.93 | 0.93 | 0.88 | 1.00 | 0.00 |
| Weight Conc. | 55.55 | 19.20 | 10.46 | 3.84 | 1.29 | 1.29 | 1.11 | 1.14 | 0.00 |

($AMG_4$)

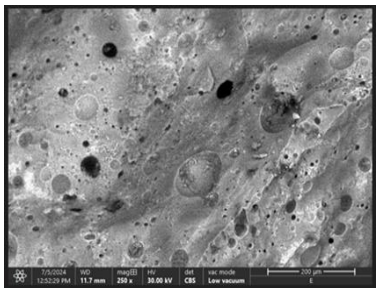

| Element symbol | Si | Na | Ca | Mg | P | K | Cl | S | Ti |
|---|---|---|---|---|---|---|---|---|---|
| Atomic Conc. | 54.36 | 27.53 | 5.80 | 5.28 | 1.15 | 0.19 | 0.59 | 1.24 | o.28 |
| Weight Conc. | 55.35 | 22.93 | 8.42 | 4.65 | 1.29 | 0.27 | 0.76 | 1.44 | 0.49 |

($AMG_5$)

Fig 3: SEM/EDS images of developed glass-ceramics system

### 3.4 Antibacterial analysis of developed glass-ceramics system

Figure 4 illustrates the antibacterial activity of glass-ceramic system produced from waste soda-lime-silica glass doped with ZnO particles. The assessment was conducted against four bacterial strains Escherichia coli, Klebsiellapneumoniae, Staphylococcus aureus, and Pseudomonas aeruginosa with bacterial inhibition quantified in colony-forming units per gram (CFU/g). The results reveal variable antibacterial efficacy across

the samples, indicating a strain-dependent response. Notably, ZnO-doped samples exhibited significantly enhanced antibacterial activity, particularly against E. coli, aligning with the widely recognized antimicrobial properties of ZnO reported in previous studies (Riaz*et al.,* 2015;Singh*et al.,* 2019; Demire*et al*., 2023). The observed variation in antibacterial response is likely due to differences in bacterial cell wall structures, metabolic processes, and sensitivity to ZnO (Lallo da Silva*et al.,* 2019; Guan*et al.,* 2021), Gram-negative bacteria, such as E. coli and Klebsiella pneumonia have been reported by Tavares *et al.,* 2020 and Tomičić*et al.,* 2020 to possess a distinct outer membrane structure compared to Gram-positive bacteria like Staphylococcus aureus and Pseudomonas aeruginosa, which can influence their interaction with ZnO and other antimicrobial agents. Furthermore, the base glass composition ($Na_2O$–CaO–$SiO_2$) may also contribute to the antibacterial activity, as the dissolution of its components in aqueous environments can release biologically active ions including $Zn^{2+}$ thereby modifying the glass-ceramic surface chemistry and enhancing its antimicrobial performance (Samad*et al.,* 2023).

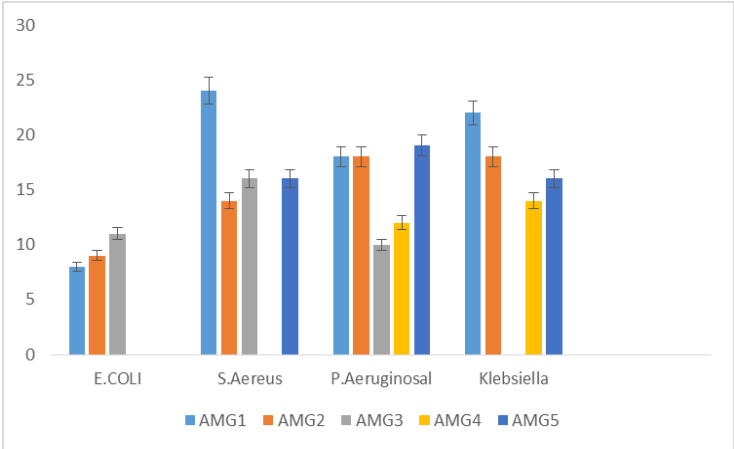


Fig 4: Antibacterial activities of developed glass-ceramics system

### 3.5 Post-in-vitro XRD analysis of developed glass-ceramics system

Figure 5 presents the post-in-vitro X-ray diffraction (XRD) analysis of glass-ceramic system developed from waste soda-lime-silica glass doped withZnO particles. The results shows that all samples, including the undoped control samples, successfully facilitated the formation of a bone-like mineral layer upon immersion in simulated body fluid (SBF), thereby confirming their bioactivity, consistent with findings reported by Hoppe *et al.,* 2011 and Hossain *et al.,* 2020. The formation of Hydroxyapatite (HA) was evident across all samples, with the characteristic HA peak intensities confirming bioactive behavior independent of ZnO doping concentrations within the studied range. The presence of ZnO diffraction peaks in the doped samples ($AMG_2$–$AMG_5$) following the in-vitro exposure suggests that a fraction of ZnO remained undissolved or untransformed during the bioactivity process. Moreover, the intensity of these ZnO peaks generally correlates positively with the initial ZnO content. Notably, the absence or markedly low intensity of HA peaks in the pre-in-vitro XRD patterns confirms that hydroxyapatite formation occurred during the in-vitro testing, substantiating the bioactivity of the materials. Furthermore, post-in-vitro changes in the intensities of crystalline phases such as combeite and wollastonite suggests their partial dissolutionoccurred tosupport the release of ions that likely contributed to HA nucleation and growth (Solonenko*et al.,* 2018; Amin *et al.,* 2021).

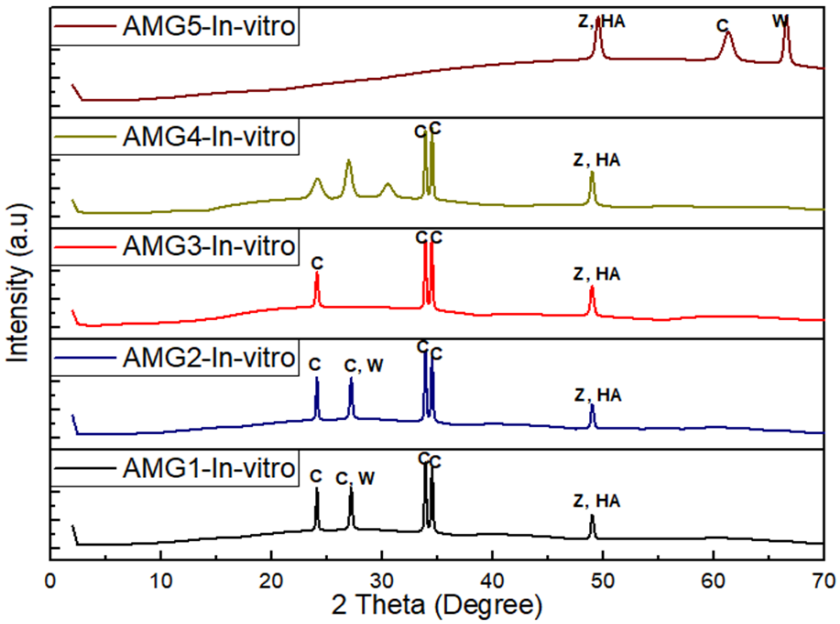


Fig. 5. Post-in-vitro XRD results of developed glass-ceramics system

### 3.6 Post-in-vitro SEM/XRF analysis of developed glass-ceramics system

Figure 6 and Table 2 present the post-in-vitro Scanning Electron Microscopy (SEM) and X-ray Fluorescence (XRF) analysis of glass-ceramic systemdeveloped from waste soda-lime-silica glass doped with ZnO particles. These analyses provide valuable insights into the surface morphology and elemental composition of the samples following immersion in simulated body fluid (SBF). The SEM micrographs reveal the presence of hydroxyapatite (HA) precipitates, observed as spherical particles or clustered formations on the sample surfaces, indicating a pronounced bioactive response (Solonenko*et al.,* 2018; Cao and Hench 1996). Complementary XRF analysis confirms a notable increase in CaO content relative to pre-in-vitro values. This compositional change supports the formation and activity of hydroxyapatite within the samples and aligns with post-in-vitro XRD results, which identified distinct HA peaks. The increased calcium content likely contributed to the development of well-defined apatite layers, as evidenced by SEM observations. Furthermore, elements such as sodium (Na) and phosphorus (P), detected in the pre-in-vitro analysis, were not observed in the post-in-vitro XRF spectra, suggesting their complete incorporation into the hydroxyapatite phase during immersion in SBF. This observation is consistent with prior reports by Hoppe *et al.,* 2011 andDash *et al.,* 2023 which highlighted the essential role of Na and P in hydroxyapatite formation

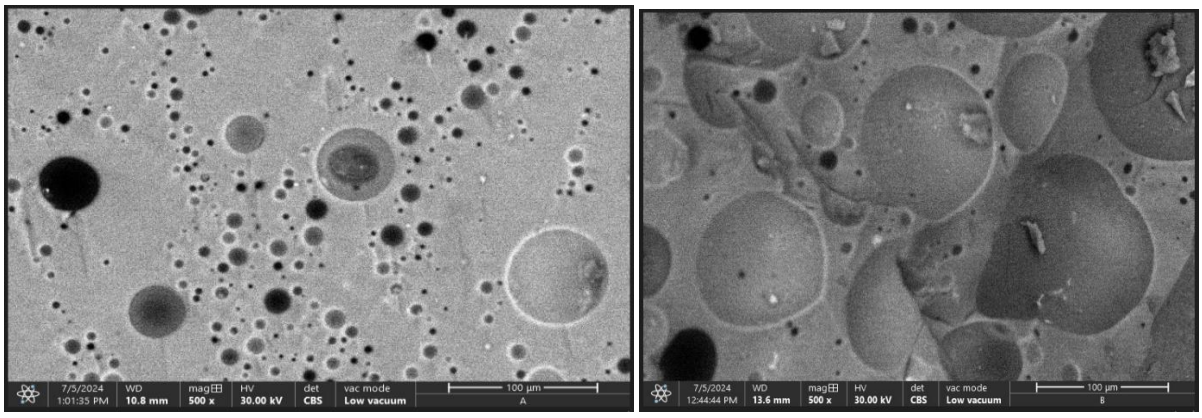

**AMG1** **AMG2**

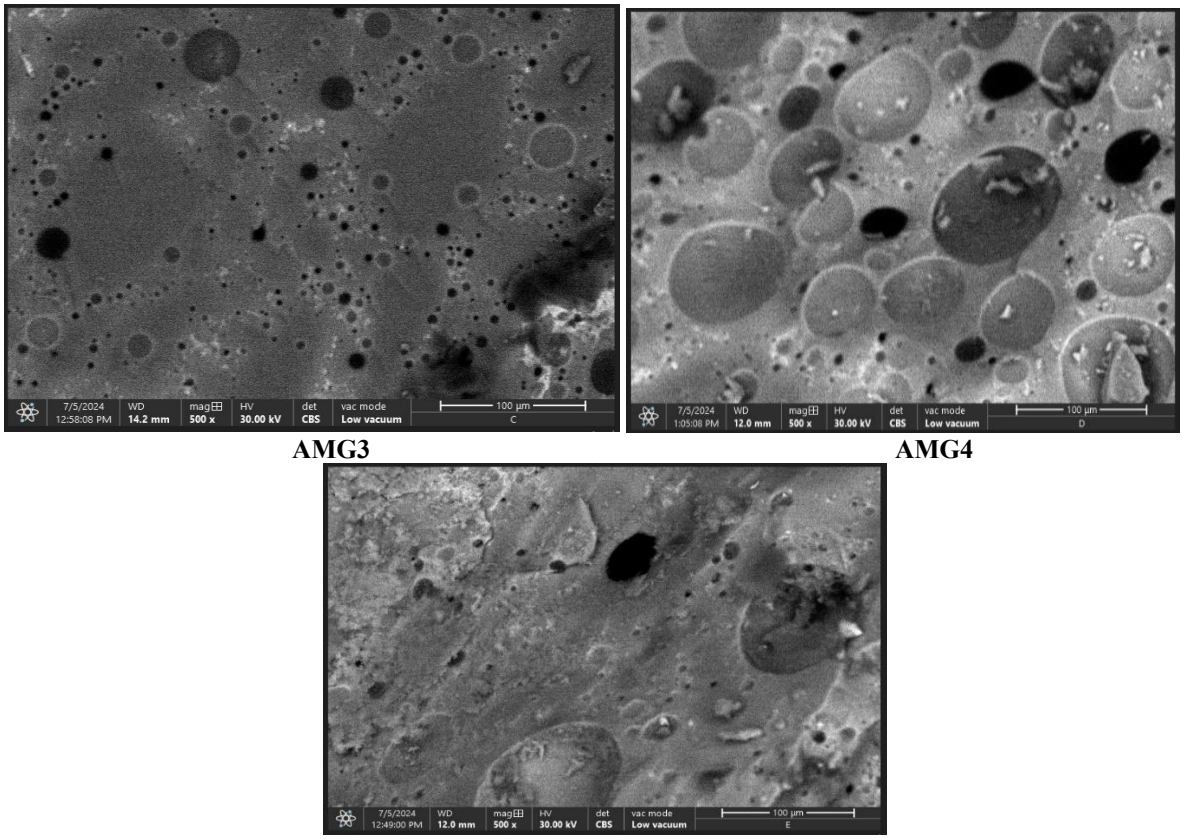


Fig. 6. Post-in-vitro SEMresults of developed glass-ceramics system

**Table 2: . XRF in-vitro analysis results of developed glass-ceramics system**

| Compositions | $SiO_2$ | Mno | Cuo | CaO | ZnO | MgO | $K_2O$ | $Al_2O_3$ | $SO_3$ | Cl |
|---|---|---|---|---|---|---|---|---|---|---|
| $AMG_1$ | 68.84 | 0.028 | 0.325 | 19.309 | - | 4.264 | 0.978 | 4.194 | 0.721 | 1.341 |
| $AMG_2$ | 53.39 | 0.016 | 0.088 | 12.630 | 24.03 | 4.469 | 0.444 | 2.908 | 0.568 | 1.457 |
| $AMG_3$ | 52.19 | 0.017 | 0.136 | 15.591 | 21.55 | 4.643 | 0.452 | 3.133 | 0.509 | 1.779 |
| $AMG_4$ | 52.39 | 0.017 | 0.126 | 16.351 | 20.09 | 4.817 | 0.488 | 3.259 | 0.544 | 1.918 |
| $AMG_5$ | 52.48 | 0.018 | 0.119 | 16.524 | 20.07 | 4.763 | 0.524 | 3.067 | 0.600 | 1.835 |

## IV. CONCLUSION

In this study, a glass-ceramic system was successfully developed and comprehensively characterized. X-ray diffraction (XRD) analysis confirmed the presence of crystalline phases such as combeite, wollastonite, and quartz in the as-prepared samples. The incorporation of ZnO was found to influence the relative intensities of these phases, which corresponded with a reduction in the mechanical properties of the materials. Scanning Electron Microscopy (SEM) further revealed microstructural modifications, particularly in particle packing density and porosity. The developed glass-ceramics also exhibited significant antibacterial activity against clinically relevant bacterial strains, primarily attributed to the release of $Zn^{2+}$ ions and the generation of reactive oxygen species, highlighting their potential for antimicrobial surface applications. Moreover, integrated XRD, SEM, and XRF analyses demonstrated excellent in-vitro bioactivity, as evidenced by the distinct emergence of hydroxyapatite (HA) peaks in the post-immersion XRD patterns peaks that were either absent or substantially weaker before immersion thereby affirming the bioactive nature and novelty of the developed materials.

## REFERENCES


[1]. Akinyele, J., Igba, U., Ayorinde, T. and Jimoh, P. (2020). Structural efficiency of burnt clay bricks containing waste crushed glass and polypropylene granules. Case Studies in Construction Materials, 13, Pp. 00404

[2]. Almasri, K. A., Matori, K. A. and Zaid, M. H. M. (2017). Effect of sintering temperature on physical, structural and optical properties of wollastonite based glass-ceramic derived from waste soda lime silica glasses. Results in physics, 7, Pp. 2242-2247

[3]. Amin, A. M., El-Amir, A. A., Karunakaran, G., Kuznetsov, D., and Ewais, E. M. (2021). In-vitro evaluation of wollastonitenano powder produced by a facile process using cheap precursors for biomedical applications. Ceramics International, 47(13), Pp. 18684-18692.

[4]. Anderson, D. M. (2010). Chief lexicographer, Dorland's Illustrated Medical Dictionary, 32nd ed., Philadelphia, PA, Elsevier Saunders. Pp.11-17.

[5]. Asokan, P., Osmani, M. and Price, A. D. (2009). Assessing the recycling potential of glass fibre reinforced plastic waste in concrete and cement composites. Journal of Cleaner Production, 17(9), Pp. 821-829

[6]. Assefi, M., Maroufi, S., Mansuri, I. and Sahajwalla, V. (2021). High strength glass foams recycled from LCD waste screens for insulation application. Journal of Cleaner Production, 280, Pp. 124-311.

[7]. Cao, W. and Hench, L. L. (1996). Bioactive materials. Ceramics international, 22(6), Pp. 493-507.

[8]. Castro, A. M., Ribeiro, M. C. S., Santos, J., Meixedo, J. P., Silva, F. J., Fiúza, A. and Alvim, M. R. (2013), Sustainable waste recycling solution for the glass fibre reinforced polymer composite materials industry. Construction and Building Materials, 45, Pp.87-94

[9]. Chanrawangyot, S., Rattanachan, S. T., Watcharenwong, A. and Fangsuwannarak, T. (2017). Antibacterial Activity of ZnO nanoparticles coated on ceramic tiles prepared by sol-gel method Journal of Metals 27(2).

[10]. Chong, F., Jianwei L., Gao Y., Abdalwahed D., Wei L., Xudong L., Baobao Z., Haidong W., Meipeng H., Lifu L. and Xin D., (2011). Recycling of waste glass as raw materials for the preparation of self-cleaning, light-weight and high-strength porous ceramics, Journal of Cleaner Production 317, Pp. 128-395

[11]. Darweesh, H. H. M. (2019). Recycling of glass waste in ceramics—part I: physical, mechanical and thermal properties SN Applied Sciences, 1:1274 https://doi.org/10.1007/s42452-019-1304-8

[12]. Dash, P. A., Mohanty, S., Nayak, S. K. (2023). A review on bioactive glass, its modifications and applications in healthcare sectors. Journal of Non-Crystalline Solids. 614: 122404

[13]. Demire, B. and ErolTaygun, M. (2023). Antibacterial borosilicate glass and glass ceramic materials doped with ZnO for usage in the pharmaceutical industry. ACS omega, 8(21), Pp. 18735-18742.

[14]. E.E. Commission, (2010). Environmental statistics and accounts in Europe, Luxembourg: Publications Office of the European Union.

[15]. Effendy, N., Sidek, H. A. A., Halimah, M. K. and Zaid, M. H. M. (2021). Enhancement on thermal, elastic and optical properties of new formulation tellurite glasses: Influence of ZnO as a glass modifier. Materials Chemistry and Physics, 273, Pp. 125156.

[16]. Guan, G., Zhang, L., Zhu, J., Wu, H., Li, W. and Sun, Q. (2021). Antibacterial properties and mechanism of biopolymer-based films functionalized by CuO/ZnO nanoparticles against Escherichia coli and Staphylococcus aureus. Journal of Hazardous Materials, 402, 123542.

[17]. Hanfi, M. Y., Sayyed, M. I., Rashad, M., Mahmoud, K. A., and Maghrbi, Y. (2024). Influence of ZnO variation on glass characteristics: Physical, mechanical properties and radiation shielding. Ceramics International, 50(24), Pp. 53073-53082

[18]. Hoppe A, Güldal N. S. and Boccaccini, A. R. (2011). A review of the biological response to ionic dissolution products from bioactive glasses and glass-ceramics. Biomaterials. 32(11): Pp. 2757-2774. https://doi.org/10.1016/j.biomaterials.2011.01.004

[19]. Hossain, S. S., Yadav, S., Majumdar, S., Krishnamurthy, S., Pyare, R. and Roy, P. K. (2020). A comparative study of physico-mechanical, bioactivity and hemolysis properties of pseudo-wollastonite and wollastonite glass-ceramic synthesized from solid wastes. Ceramics International, 46(1), Pp. 833-843.

[20]. Hussein H, Alyaa A., Bassam T., Fadzil Y. and Blessen T. (2022). Effect of recycled waste glass on the properties of high-performance concrete: A critical review, Case Studies in Construction Materials 17, 01149

[21]. Hsiang, H. I., Chen, C. C. and Yang, S. Y., (2019). Microwave dielectric properties of Ca0.7Nd0.2TiO3 ceramic-filled CaO-B2O3-SiO2 glass for LTCC applications. J. Adv. Ceram. 8, Pp.345–351.

[22]. Idejan, G., Lima, A. l., Sousa, E., Souza, M., Cunha-Filho, M., Silva, I., Orsi, D. and Sá-Barreto, L. (2024). Antimicrobial and acaricide sanitizer tablets produced by wet granulation of spray-dried soap and clove oil-loaded micro emulsion. PLOS ONE. 19

[23]. Jani, Y. and Hogland, W. (2014). Waste glass in the production of cement and concrete–a review, J. Environ. Chem. Eng. 2, Pp.1767–1775.

[24]. Kim, D. A., Abo-Mosallam, H., Lee, H. Y., Lee, J. H., Kim, H. W., and Lee, H. H. (2015). Biological and mechanical properties of an experimental glass-ionomer cement modified by partial replacement of CaO with MgO or ZnO. Journal of applied oral science, 23(4), Pp. 369-375.

[25]. Kokubo, T. and Takadama, H. (2006). How useful is SBF in predicting in vivo bone bioactivity? Biomaterials 27, Pp. 2907–2915

[26]. Lallo da Silva, B., Abuçafy, M. P., BerbelManaia, E., Oshiro Junior, J. A., Chiari-Andréo, B. G., Pietro, R. C. R. and Chiavacci, L. A. (2019). Relationship between structure and antimicrobial activity of zinc oxide nanoparticles: An overview. International journal of nanomedicine Pp. 9395-9410.

[27]. Li, C. Y., Li, G. B., Ouyang, H. B. and Lu, J., (2019). ZrB2 particles reinforced glass coating for oxidation protection of carbon/carbon composites. J. Adv. Ceram. 8, Pp. 102–111.

[28]. López, F. A., Martín, M. I., García-Díaz, I., Rodríguez, O., Alguacil, F. J., and Romero, M. (2012). Recycling of glass fibers from fiberglass polyester waste composite for the manufacture of glass-ceramic materials. Journal of Environmental protection, 3(8), 740-747

[29]. Mahboubizadeh1, S., Noroozi, P. and Ashkani, O. (2023). Bioactive Glass in Medicine: A Mini-Review of Composition, Properties, Bioactivity Mechanisms, and Clinical Applications, Journal of Environmental Friendly Materials, Vol. 7, No. 2, Pp. 65-70.

[30]. Mahdy, M. A., El Zawawi, I. K., Kenawy, S. H., Hamzawy, E. M. and El-Bassyouni, G. T. (2022). Effect of zinc oxide on wollastonite: Structural, optical, and mechanical properties. Ceramics International, 48(5), Pp. 7218-7231

[31]. Maryan, I. E., Nurjanah, N. S., Hadisantoso, E. P. and Wijayanti, R. B. (2020). The Effect of TiO2 additives on the antibacterial properties (Escherichia coli and Staphylococcus aureus) of glaze on ceramic tiles, Materials Science and Engineering 980, 012011 doi:10.1088/1757-899X/980/1/012011

[32]. Matori, K. A., Zaid, M. H. M., Sidek, H. A. A., Halimah, M. K., Wahab, Z. A. and Sabri, M. G. M. (2010). Influence of ZnO on the ultrasonic velocity and elastic moduli of soda lime silicate glasses. International Journal of Physical Sciences, 5(14), Pp. 2212-2216.

[33]. Mio, M., Perero, S., Ferraris, S., Battiato, A., Manfredotti, C., Vittone, E., Vento, D. D, Vada, S. V., Fucale, G. and Ferraris, M. (2014). Silver nanocluster-silica composite antibacterial coating for materials to be used in mobile telephones Applied Surface Science 313 Pp.107-125

[34]. Noguera J. F., Moreno A., Gozalbo A. and Orts M. J. (2010). Development of ceramic glaze compositions with bactericidal and fungicidal properties Qualicer'10 Castellon (Spain).

[35]. Onaizi, S. A. and Leong, S. S. (2011). Tethering Antimicrobial Peptides. Biotechnology. Advances, 29: Pp. 67-74.

[36]. Özcan, S., Açikbaş, N. C. and Açikbaş, G. (2017). Formation of antibacterial effect on ceramic tile surfaces Anadolu University Journal of Science and Technology A- Applied Sciences and Engineering, VoL: 18 No: 1, Pp. 122 – 130

[37]. Pahlevani, F. and Sahajwalla, V. (2018). From waste glass to building materials–An innovative sustainable solution for waste glass. Journal of cleaner production, 191, Pp. 192-206.

[38]. Riaz, M., Zia, R., Saleemi, F., Ikram, H. and Bashir, F. (2015). In vitro antimicrobial activity of ZnO based glass–ceramics against pathogenic bacteria. Journal of Materials Science: Materials in Medicine, 26, Pp. 1-12.

[39]. Robert, D., Baez, E. and Setunge, S. (2021). A new technology of transforming recycled glass waste to construction components. Construction and Building Materials, 313, Pp. 125-539.

[40]. Sahu, P., Ali, S. M., Shenoy, K. T., Arvind, A., Sugilal, G. and Kaushik, C. P. (2023). Combined experiments and atomistic simulations for understanding the effect of ZnO on the sodium silicate and sodium borosilicate glass network. Journal of Non-Crystalline Solids, 618, 122550.

[41]. Samad, H. A. and Nurddin, S. M. A. S. M. (2023). Development of Bioactive Glass Ceramics Based on SiO2-CaO-Na2O-P2O5 System using Limestone and Silica Sand as Starting Materials. Journal of Research in Nanoscience and Nanotechnology, 9(1), Pp. 54-64.

[42]. Singh, G., Kumar, S., Singh, V. P. and Vaish, R. (2019). Transparent ZnO crystallized glass ceramics for photocatalytic and antibacterial applications. Journal of Applied Physics, 125(17).

[43]. Soares, V. O., Daguano, J. K., Lombello, C. B., Bianchin, O. S., Gonçalves, L. M. and Zanotto, E. D. (2018). New sintered wollastonite glass-ceramic for biomedical applications. Ceramics International, 44(16), Pp. 20019-20027

[44]. Solonenko, A. P., Blesman, A. I. and Polonyankin, D. A. (2018). Preparation and in vitro apatite-forming ability of hydroxyapatite and β-wollastonite composite materials. Ceramics International, 44(15), Pp. 17824-17834.

[45]. Tavares, T. D., Antunes, J. C., Padrão, J., Ribeiro, A. I., Zille, A., Amorim, M. T. P. and Felgueiras, H. P. (2020). Activity of specialized biomolecules against gram-positive and gram-negative bacteria. Antibiotics, 9(6), 314.

[46]. Thipperudrappa, S., UllalKini, A. and Hiremath, A. (2020). Influence of zinc oxide nanoparticles on the mechanical and thermal responses of glass fiber-reinforced epoxy nanocomposites. Polymer Composites, 41(1), Pp. 174-181

[47]. Tomičić, R., Tomičić, Z., Thaler, N., Humar, M. and Raspor, P. (2020). Factors influencing adhesion of bacteria Escherichia coli, Pseudomonas aeruginosa, Staphylococcus aureus and yeast Pichiamembranifaciens to wooden surfaces. Wood Science and Technology, 54, Pp. 1663-1676.

[48]. Wang, T.H., (2020). Key Figures on Glass Recycling Worldwide as of 2018 (accessed February, 2nd). https://www.statista.com/statistics/1055604/key-figures-glass-recycling-globally/#statisticContainer.